https://doi.org/10.1016/j.biomaterials.2018.06.008

Mussel-inspired catalytic selenocystamine-dopamine coatings for long-term generation of therapeutic gas on cardiovascular stents

Zhilu Yang ***[a]; Ying Yang[a]; Li Zhang[b]; Kaiqin Xiong[a]; Xiangyang Li[a]; Feng Zhang[a]; Jin Wang[a]; Xin Zhao**[b]; Nan Huang*[a]

a

Key Lab. of Advanced Technology for Materials of Education Ministry, School of Materials Science and Engineering, Southwest Jiaotong University, Chengdu, 610031, China

b

Department of Biomedical Engineering, The Hong Kong Polytechnic University, Hung Hom, Kowloon, Hong Kong, China

Abstract

The development of a nitric oxide (NO)-generating surface with long-term, stable and controllable NO release improves the therapeutic efficacy of cardiovascular stents. In this work, we developed a “one-pot” method inspired by mussel adhesive proteins for copolymerization of selenocystamine (SeCA) and dopamine (Dopa) to form a NO-generating coating on a 316 L stainless steel (SS) stent. This “one-pot” method is environmentally friendly and easy to popularize, with many advantages including simple manufacturing procedure, high stability and no involvement of organic solvents. Such SeCA/Dopa coatings also enabled us to develop a catalytic surface for local NO-generation by reaction of endogenously existing S-nitrothiol species from fresh blood. We found that the developed SeCA/Dopa coatings could release NO in a controllable and stable manner for more than 60 days. Additionally, the released NO significantly inhibited smooth muscle cell (SMC) proliferation and migration, as well as platelet activation and aggregation through the up-regulation of cyclic guanosine monophosphate synthesis. Moreover, such NO generation enhanced the adhesion, proliferation and migration of endothelial cells (ECs), and achieved rapid in vivo re-endothelialization, effectively reducing in-stent restenosis and neointimal hyperplasia. We envision that the SeCA/Dopa-coated 316 L SS stent could be a promising platform for treatment of cardiovascular diseases.

Graphical abstract

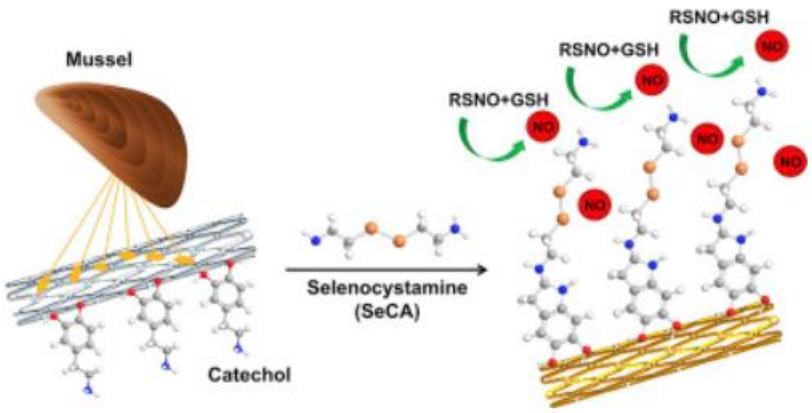

1. Introduction

Coronary artery disease (CAD) is a major cause of morbidity worldwide, accounting for 7.4 million deaths and over USD $300 billion healthcare costs per year [1,2]. Cardiovascular stents such as the drug eluting stents (DES) [3] and Genous™ endothelial progenitor cell (EPC) capturing stents [4] have been invented to clinically treat CAD. Unfortunately, implantation of these cardiovascular stents will activate the inflammatory and vascular repair responses, and induce migration and proliferation of smooth muscle cells (SMCs) as well as the adhesion of blood platelets, leading to in-stent restenosis (ISR), late stent thrombosis (LST) and delayed re-endothelialization, thereby reducing their long-term success in clinic [5,6].

To improve the clinical performance of cardiovascular stents, modification of the stent surfaces using biomolecules/drugs such as vascular endothelial growth factor (VEGF) [7], anti-CD34 antibodies [8], paclitaxel [9] and nitric oxide (NO)-releasing molecules [10] to control the behaviors of endothelial cells (ECs), platelets and SMCs have been developed. Among these biomolecules, NO, a cell signaling molecule endogenously synthesized by ECs, has been proposed as a promising candidate thanks to its key role in regulating platelet aggregation [11], SMC proliferation [12] and endothelial progenitor cell (EPC) behaviors such as mobilization and differentiation [13]. The lack of NO around the implanted stents will lead to ISR and LST [14], yet excessive amounts of NO may imply a greater degree of interactions with superoxide (O_2^-) to form peroxynitrites ($ONOO^-$), which might be harmful for re-endothelialization of damaged arterial segments in vivo (re-endothelialization is crucial to maintain vascular homeostasis) [15,16]. To control the NO release, several attempts have been made by incorporating NO donors into various matrixes, including polymeric microparticles [17], polymers [18], and liposomes [10] through blending or covalent linkage. These approaches unfortunately suffer from drawbacks including burst or insufficient NO release and inevitable cytotoxicity [19]. Furthermore, most covalent linkage methods on a material surface currently available for clinical use involve complex multi-step processes associated with pre-treatments to introduce functional groups and covalent immobilization procedures to materials. Therefore, strategies allowing for facile and on-demand NO generation over a prolonged period are highly sought after.

Herein, we propose a strategy that employs NO donor molecules from blood itself for a local and sustained delivery of NO. We developed a material-independent, one-step, dip-coating approach to continuously produce the therapeutic gas NO from a stent by incorporating glutathione peroxidase (GPx) at the solid interface via co-immobilization of selenocystamine (SeCA) in the framework of dopamine (Dopa). Such SeCA/Dopa coatings will enable us to develop a catalytic surface for local NO-generation, which is likely to be maintained for an extended time period by reaction of endogenously existing S-nitrothiol (RSNO) species in fresh blood. The amount of generated NO can be controlled within a physiological level of 0.5–4×10^{-10} mol $cm^{-2} \cdot min^{-1}$ by controlling the concentration of SeCA, ultimately leading to a surface-modified cardiovascular stent to promote re-endothelialization and reduce restenosis and thrombosis. Without tedious multi-step syntheses and involvement of toxic chemicals during synthesis, our simple and biocompatible SeCA/Dopa coating will demonstrate an on-demand and facile dose control of NO generation from the functionalized stent surfaces. We envision that the catalytic SeCA/Dopa surface chemistry has wide applications in the field of

blood-contacting devices.

2. Materials and methods

2.1. Preparation of NO generating SeCA/Dopa coatings

SeCA/Dopa coatings were fabricated through the dip-coating of planar substrates, including 316 L stainless steel (SS), cobalt-chromium (CoCr), and Nitinol (NiTi) alloys (commonly used metal materials for vascular stents) and 316 L SS cardiovascular stents. The wafers of mirror-polished 316 L SS, CoCr and NiTi with a size of 1 cm × 1 cm and 316 L SS cardiovascular stent with a size of Φ1.65 mm × 18 mm were ultrasonically cleaned by acetone, ethylalcohol and ultrapure water before use. Replacing acetone with HCl, polyethylene terephthalate (PET) wafers were cleaned using the same method. To obtain SeCA/Dopa coatings with a controllable NO release rate, SeCA and dopamine hydrochloride with molar ratios ranging from 0.1:1 to 2:1 were used to produce NO-generating coatings, where dopamine hydrochloride was kept at a constant concentration of 0.25 mg/mL. In detail, SeCA and dopamine hydrochloride were dissolved in 10 mM Tris-HCl (pH 8.5), and the planar substrates of 316 L SS, CoCr, and NiTi were subsequently dipped into the reaction solution mentioned above. The coated planar substrates were ultrasonically washed with distilled water and dried by N2 gas. 0.84 mg/mL of SeCA and 0.25 mg/mL of dopamine hydrochloride (corresponding to the molar ratio of 2:1 of SeCA to dopamine hydrochloride) were dissolved in 10 mM Tris-HCl (pH 8.5) and filled in a 2 mL tube. The 316 L SS cardiovascular stent was soaked in the above reaction solution for 12 h to allow for the formation of the SeCA/Dopa coating. The coated stents were then ultrasonically washed with distilled water and dried using N2 gas.

2.2. NO generation from SeCA/Dopa coatings

Chemiluminescence was performed using NO analyzer (NOA) (Seivers 280i, Boulder, CO) to monitor the release of NO induced by the SeCA/Dopa coatings in real time. Here, a 316 L SS foil (0.5 × 1 cm) was used for the deposition of SeCA/Dopa coating. S-nitroso-N-acetylpenicillamine (SNAP), a common endogenous RSNO species, was used for the evaluation of NO generation. 5 mL of test solution consisting of 10 μM SNAP, 10 μM glutathione (GSH) and 500 μM ethylenediaminetetraacetic acid (EDTA) (to prevent metal-ion induced SNAP decomposition) dissolved in PBS (pH 7.4) was added into a reaction flask, and the SeCA/Dopa-coated foil was soaked into the solution. The NO generated from the catalytic SNAP decomposition was purged from the test solution and transported to the NOA by a stream of N2 gas. The amount of NO induced by the SeCA/Dopa-coating was calculated according to the calibration curves of the NOA, as detailed in literature [20]. The remaining Se on the surface and inside the coating (2 nm from the edge, generated via 3 s of Ar etching) was monitored at predetermined time points using X-ray photoelectron spectroscopy (XPS).

2.3. Test of adhesion, activation and cyclic guanylate monophosphate (cGMP) synthesis of platelets

Human platelet rich plasma (PRP) obtained from the central blood station of Chengdu, China was used in this study following ethics standards. Considering the poor chemical stability of RSNO and the resulting deficiency of endogenous RSNO preserved in PRP, a moderate

amount of RSNO consisting of 10 μM SNAP and 10 μM GSH was supplemented in PRP for the in vitro platelet test. Additionally, 10 μL collagen I-solution (50 μg/mL, dissolved in 3% glacial acetic acid) was added for the collagen activation assay. The test samples were incubated in PRP for 30 min then subsequently removed. Next, the samples were thoroughly washed with PBS and soaked in 2% glutaraldehyde for 12 h. After further dehydration and de-alcoholization, the samples were gold sputtered and observed by scanning electron microscopy (SEM, Quanta 200, FEI, Holland). Synthesis of cGMP platelets adhering to samples was determined by a human cGMP Enzyme-Linked ImmunoSorbent Assay (ELISA) kit. Similar to the platelet adhesion experiment, each sample was incubated in 1 mL PRP supplemented with NO donor and collagen I solution for 30 min 100 μL of 10% triton-X was added into PRP and sonicated. The PRP was centrifuged at 2500 rpm to separate the cell fragments, and the supernatant was used for cGMP analysis.

2.4. Adhesion, proliferation and cGMP synthesis of SMCs

To simulate the in vivo environment in a cardiovascular system, culture of human umbilical artery smooth muscle cells (HUASMCs) was performed using cell culture media supplemented with a moderate NO donor (10 μM SNAP, 10 μM GSH). Briefly, HUASMCs were cultured on samples at a density of 5 × 104 cells/cm2. For day 1 and 3 of culture, NO donor was supplemented in cell culture medium every 4 h. Cell Counting Kit-8 (CCK-8) was used to evaluate cell proliferation, and fluorescence staining was employed to evaluate cell morphology [21]. Analysis of cGMP synthesized by HUASMCs after 2 h of culture on samples was performed using human cGMP ELISA kit, where the test procedure was similar to the platelets.

2.5. Proliferation of ECs

Like the HUASMC culture, human umbilical vein endothelial cells (HUVECs) were seeded on samples at a density of 5 × 104 cells/cm2. During incubation, NO donor (10 μM SNAP, 10 μM GSH) was supplemented in cell culture media every 4 h. After 1 and 3 days of culture, cells were stained with phalloidin conjugated to tetramethyl rhodamine isothiocyanate (TRITC) (Sigma-Aldrich) to examine cell adhesion. Furthermore, CCK-8 was used to evaluate cell proliferation according to the manufacturer's instructions.

2.6. Migration of ECs and SMCs

HUVECs or HUASMCs were seeded on test samples at a density of 5 × 105 cells/cm2 for 6 h to form an intact cell layer to simulate the status of ECs and SMCs in natural blood vessels. Briefly, the 316 L SS foil (15 cm × 10 cm) was dipped halfway with the SeCA/Dopa coating. When the naked half of the 316 L SS foil was covered by a confluent cell layer after 6 h of culture, the sample was vertically turned over and transferred to a well plate filled with new culture medium supplemented with the NO donor. The cells were incubated for another 24 h. During cell incubation, NO donor (10 μM SNAP, 10 μM GSH) was supplemented in the cell culture media every 4 h. The cells were stained with rhodamine, and the migration of cells on the half SeCA/Dopa-modified samples was observed using a Leica DMRX fluorescence microscope.

2.7. Co-culture of ECs and SMCs

Co-culture of HUVECs and HUASMCs was performed to evaluate the competitive behaviors of the two cell types. Briefly, HUASMCs were pre-labelled with Orange CMTMR, while HUVECs were pre-labelled with Cell Tracker Green CMFDA according to product instructions (Molecular Probes/ThermoFisher, Oregon, USA). The fluorescently labelled HUASMCs and HUVECs were isolated by 0.25% trypsin-EDTA solution and centrifuged at 1200 rpm for 5 min. After the HUVECs and HUASMCs were re-suspended separately in DMEM/F12 medium with 10% fetal bovine serum at a concentration of 5 × 104 cells/mL, their suspensions were mixed in a volume ratio of 1:1 and then seeded on samples at a density of 5 × 104 cells/cm2. After co-culture for 2 h in an incubator at 37 °C humidified air with 5% CO2, the cells were observed by a Leica DMRX fluorescence microscope. The number of attached cells was calculated from at least 12 images.

2.8. Thrombogenicity in ex vivo circulation

All procedures were compliant with the China Council on Animal Care and Southwest Jiaotong University animal use protocol, following all ethical guidelines for experimental animals. Six New Zealand white rabbits (2.5–3.5 kg) were used in this work. Experiments were carried out under general anesthesia. The left carotid artery and the right jugular vein of rabbits were isolated, and the AV extracorporeal circuit (ECC) was connected by cannulating the left carotid artery and right external jugular vein. Commercially available polyvinyl chloride (PVC) cardiopulmonary perfusion tubing with internal installation of SeCA/Dopa-modified 316 L SS foil was assembled into a New Zealand white rabbit arteriovenous shunt. The 316 L SS foil (0.8 mm × 1 mm) before and after SeCA/Dopa modification was first curled and tightly affixed onto the inner wall of the PVC cardiopulmonary perfusion tubing. The arterial and venous sides of the ECC were unclamped, and the blood flow in the circuit was monitored for 2 h. The circuit was then stopped and removed from the animal and rinsed with PBS (pH 7.4). Cross-sections of the tubes containing implanted samples were photographed for analysis of the percentage of occlusion of circuits. The residual thrombosis in the tube around the implanted samples was collected, photographed and weighed. The specimen was taken out and rinsed with PBS (pH 7.4) and fixed in 2.5% glutaraldehyde solution overnight. Specimens were observed by SEM after dehydration, de-alcoholization and critical point drying.

2.9. In vivo stent implantation and characterization

8 adult New Zealand white rabbits weighing 3.5–4.0 kg and 16 cardiovascular stents were used. The rabbits were divided into two groups: the control 316 L SS stents and the SeCA/Dopa-coated 316 L SS stents. Two stents from each group were respectively implanted bilaterally in the iliac arteries of a rabbit with the aid of angiography. Stent implantation in rabbit iliac arteries without systemic heparin anticoagulation was performed for 1 and 3 months. Following 1 and 3 months of implantation, the animals were anaesthetized for angiography to confirm the patency of the iliac artery. Half of the stented arteries were cut open lengthwise and fixed with 2.5% glutaraldehyde in PBS. After dehydration, de-alcoholization and critical point drying, these stented arteries were observed using SEM. The other stented arteries were fixed with 10% formaldehyde in PBS and used for tissue slicing analysis. Cross-sectional slices were stained using Van Gieson's Staining protocol for histomorphometric analysis.

The surface elemental composition of SeCA/Dopa coating was measured using XPS. The instrument (Kratos, Axis Ultra DLD) was equipped with a monochromatic Al Kα (hν = 1486.6 ev) X-ray source operated at 15 kV, 150 W and a pressure of 2 × 10−7 Pa. Atomic percentages of various elements were derived from broad range spectra, using the Al source in a low-resolution mode (pass energy 160 eV), while a pass energy of 20 eV was used for high-resolution spectra. The C1s peak (binding energy 285.0 eV) was used as a reference for charge correction.

The thickness of the coating was analyzed by a spectroscopic ellipsometer (M − 2000V, J.A. Woollam, USA). The data analysis was based on Δ and Ψ values measured at a wavelength of 370–1000 nm, and the Cauchy model was used to calculate the coating thickness. Analysis of the mean size and size distribution of the SeCA/Dopa particles in reaction solution after dip-coating in planar substrate for 12 h was performed by a Malvern Zeta-sizer Nano-ZS90 (Malvern, UK). Atomic force microscopy (AFM, SPI 3800, NSK Inc., Japan) was employed to analyze the surface morphology and roughness. Intermittent contact mode with the scan frequency of 5 Hz was chosen to observe the topography of SeCA/Dopa-coated planar substrate.

To explore the polymerization mechanisms of SeCA/Dopa, matrix-assisted laser desorption/ionization (MALDI) mass spectroscopy (MALDI MS) spectrum was analyzed. MALDI MS measurement was performed with a MALDI micro MX time-of-flight mass spectrometer (Waters, Milford, MA) operated in the reflection mode. The MALDI source is equipped with a 337 nm N2 laser operated with 4 ns-duration pulses. The laser pulse energy was set as 200 arbitrary units (AU) when using 2,5-dihydroxybenzoic acid (DHB) as the matrix. The MS spectra were recorded in the range of 50–4000 m/z. Each MS spectrum consisting of average ions from ten laser shots and 10 mass spectra were combined for the data analysis of each sample. The matrix solutions were prepared by dissolving DHB in 1:4 (v/v) 0.1% trifluoroacetic acid (TFA)/acetonitrile at a concentration of 20 mg/mL. For MALDI analysis of SeCA/Dopa coating, the MALDI target plate (stainless steel) was directly modified by SeCA/Dopa coating. 1 μL of the DHB matrix solution was added to the SeCA/Dopa-modified plate and air dried prior to further use.

To determine the mechanical properties of the SeCA/Dopa coating used for cardiovascular stent modification, balloon dilatation tests were employed. The SeCA/Dopa-coated 316 L SS cardiovascular stent (1.65 mm × 18 mm) was mounted onto an angioplasty balloon using a stent crimper. The balloon was dilated to 3 mm (diameter) at a pressure of 9 × 105 Pa. Surface morphology of the post-expansion stent was observed by field emission SEM (JSM-6390, JEOL, Japan) to evaluate the mechanical properties of the SeCA/Dopa coating.

2.10. Statistical analysis

Parallel experiments were designed for all blood, cell, ex vivo and in vivo assays and repeated three times. The data were presented as means ± standard error (SE). Statistically analysis was carried out as one-way ANOVA, while *$p < 0.05$ suggesting significant difference.

3. Results and discussion

3.1. Characterization of SeCA/Dopa coatings

The design of the SeCA/Dopa coating was inspired by the Mytilus edulis that attaches to

solid substrates via byssal threads and adhesion plaques consisting of levodopa (L-DOPA) and lysine, two important molecules in the foot protein 5 (Mefp-5) for adhesion to a wide spectrum of materials (Fig. 1A(i-iii)) [22]. L-DOPA is the bio-inspired building block for surface adhesion coatings, and lysine is a part of the SeCA protein (Fig. 1A (iv-v)). The SeCA/Dopa coatings on 316 L SS stents were developed through one-step dip-coating in an alkaline aqueous solution consisting of SeCA and Dopa, buffered by 10 mM Tris to a pH of 8.5. To prepare the NO-generating coatings with adjustable and controllable release rates, various SeCA-to-Dopa molar ratios of 0.1:1, 0.5:1, 1:1 and 2:1 were explored. One-step immersion of substrates in SeCA/Dopa reaction solutions for 12 h resulted in a spontaneous deposition of the thin adherent co-polymerized SeCA/Dopa coatings, with thickness ranging from 9.1 to 16.1 nm (Fig. 1B) and with root-mean-square (RMS) from 10.1 to 29.2 nm (Fig. S1, Supporting Information). The chemistry of the Schiff-base formation and Michael addition between amine and catechol groups were confirmed by the MALDI-MS. The peaks of [M+H]+ ions at 376, 393, 397 and 545 m/z were clearly present during polymerization (Fig. S2), indicating the presence of the crosslinking reactions between Dopa and SeCA via the assembling process. The XPS analysis of the SeCA/Dopa coatings revealed the absence of specific elements including Ni, Fe, and Cr of 316 L SS, suggesting the formation of compact coatings (Fig. 1C). The content of Se in the SeCA/Dopa coating increased with an increasing SeCA-to-Dopa molar ratio as expected (Fig. 1C, Fig. S3, Table S1). Moreover, such SeCA/Dopa coatings could be universally formed on diverse types of materials with little variation in the atomic composition (Fig. 1C, Fig. S4, Table S2). It is worth noting that there was no significant difference in the atomic composition of Se, and the Se/N ratio of SeCA/Dopa (2:1) coatings formed at different deposition times from 4 to 48 h (Fig. 1D), suggesting the uniform distribution of Se in the SeCA/Dopa coating. The above results have indicated that the formation of SeCA/Dopa coating on the cardiovascular stents via co-immobilization of SeCA and Dopa was successful.

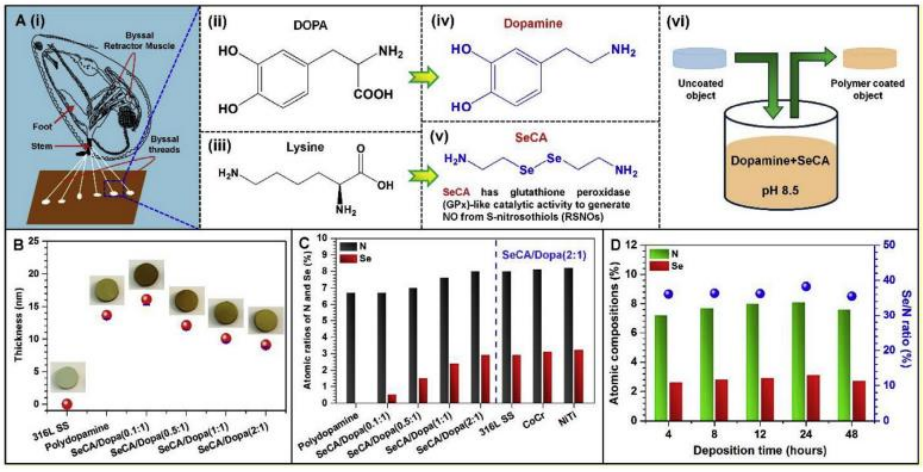

Fig. 1. Formation and characteristics of SeCA/Dopa coating. (A) Mussel-inspired chemistry for designing SeCA/Dopa coating: (i) Schematic diagram of the *Mytilus edulis* attaching to solid substrates via byssal threads and adhesion plaques; (ii and iii) The chemical structures of the L-DOPA and lysine; (iv and v) The chemical structures of the dopamine and SeCA; (vi) Schematic illustration of the NO-generating coating deposition by dip-coating in an alkaline SeCA/dopamine solution. (B) Images and thicknesses of the control 316 L SS substrate before and after coating with polydopamine, SeCA/Dopa (0.1:1), SeCA/Dopa (0.5:1), SeCA/Dopa (1:1), and SeCA/Dopa (2:1). (C) The atomic compositions of N and Se of polydopamine, SeCA/Dopa (0.1:1), SeCA/Dopa (0.5:1), SeCA/Dopa (1:1), and SeCA/Dopa (2:1) deposited on 316 L SS substrate (left) and SeCA/Dopa (2:1) coatings deposited on various substrates (right). (D) Change of atomic compositions and Se/N ratio of SeCA/Dopa (2:1) coating with time.

3.2. Analysis of stent dilation and NO generation induced by SeCA/Dopa coatings

Cardiovascular stents undergo rigorous and complex distortion when mounted onto an angioplasty balloon and dilated to target size after implantation. Therefore, the adhesion strength of

the coating to the substrate is crucial for its performance in vivo [23,24]. To investigate the adhesion strength of the SeCA/Dopa coating on 316 L SS cardiovascular stents, a stent dilation analysis was performed. The results demonstrated that the SeCA/Dopa coating was compact and homogeneous, with no appearance of cracks or peeling after a balloon dilation with an increase of 81.8% in diameter (Fig. 2A and B). These results have suggested that the SeCA/Dopa coating is flexible enough to withstand deformation during the balloon dilation procedure.

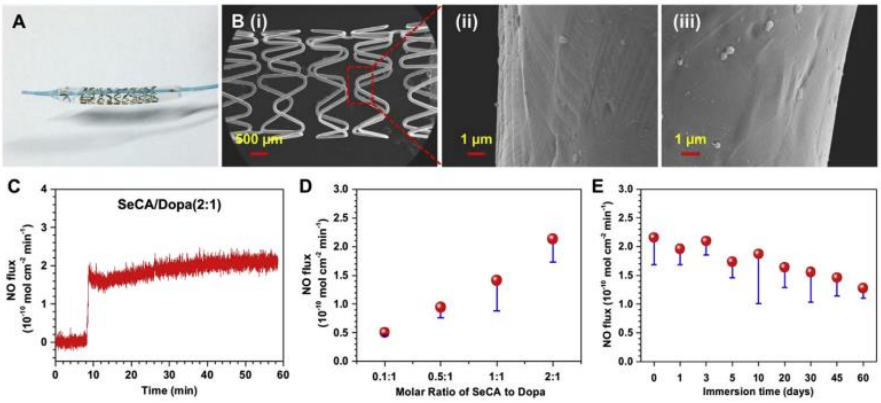

Fig. 2. Macro and microscopic images and NO generating capability of resultant SeCA/Dopa coating. (A) Representative image of a SeCA/Dopa-coated 316 L SS stent mounted onto a dilated angioplasty balloon. (B) Representative SEM micrographs of the 316 L SS stent coated with SeCA/Dopa after dilation. Note that the coating on the stent was homogeneous with no cracks. (C) Catalytic NO generation pattern with time induced by SeCA/Dopa (2:1) in PBS containing NO donor. (D) Calculated release rates of NO generated by SeCA/Dopa (0.1:1), SeCA/Dopa (0.5:1), SeCA/Dopa (1:1) and SeCA/Dopa (2:1) coatings respectively. (E) NO generation induced by SeCA/Dopa (2:1) after continuous exposure to PBS containing NO donor.

A real-time chemiluminescent assay was next performed to examine the in vitro NO release behavior of the SeCA/Dopa coating on 316 L SS substrates. NO release rates from the coatings with different SeCA/Dopa molar ratios were tested in a deoxygenated PBS solution (pH 7.4) supplemented with 10 μM SNAP, 10 μM GSH, and 500 μM EDTA. NO generation was found to start as soon as 10 min after PBS immersion (Fig. 2C). Real-time monitoring of NO production from the SeCA/Dopa coatings revealed a dose-dependent manner of SeCA immobilization: a high SeCA/Dopa molar ratio resulted in an increased NO flux (Fig. 2D). We could also control the NO release rates from 0.5 to 2.2 × 10−10 mol cm−2·min−1, which lie well within the range of the natural endothelium environment (0.5–4 × 10−10 mol cm−2·min−1) via simply regulating the SeCA-to-Dopa molar ratio [25]. In addition, the SeCA/Dopa coatings showed excellent long-term NO generation for 60 days (Fig. 2E). After continuous exposure to the NO donor solution for 60 days, the SeCA/Dopa coatings maintained 55% of the NO production rate of an initiative SeCA/Dopa coating. This may be attributed to the excellent retention of Se content in the coating; we found that the retention of Se content on the surface and inside the coating (2 nm from the edge) was as high as 81% and 86%, respectively, after 60 days of PBS exposure (Fig. S5A and B). This exceptional long-term NO generation system clearly outcompetes existing methods, which provided NO for 30 days with significant content loss [24,26]. Consequently, controllable, stable and long-term continuous release of NO flux can be achieved using our catalytic SeCA/Dopa coatings, indicating its long-term efficacy as a coating for blood contacting devices.

3.3. Effects of SeCA/Dopa coatings on behaviors of platelets, SMCs and ECs

We further evaluated the biological effects of our catalytic NO-generating coatings on adhesion, proliferation and/or migration of platelets, SMCs and ECs, as these cells play an important role in major clinical complications of cardiovascular stents like ISR and LST. We first examined the effects of SeCA/Dopa coatings on adhesion of platelets and expression of cGMP, as NO could

suppress platelet adhesion via cGMP signaling pathway [27,28]. We seeded the PRP onto the substrate surface of 316 L SS, polydopamine or SeCA/Dopa coatings at different SeCA/Dopa molar ratios in the absence or presence of NO donor, i.e., RSNO, consisting of SNAP (10 μM), GSH (10 μM) and collagen (50 μg/mL). We found that the SeCA/Dopa-coated surface effectively inhibited platelet adhesion (Fig. 3A) and promoted cGMP expression (Fig. 3B) in the presence of NO donor, whereas in the absence of NO donor the platelets could adhere to the SeCA/Dopa coatings and exhibited a spread morphology (Fig. S6). Increase in the SeCA/Dopa molar ratio resulted in enhanced inhibition and cGMP expression (Fig. 3A and B). These results suggested that the SeCA/Dopa coatings can catalyze NO generation in the presence of NO donor and inhibit platelet adhesion by activating the expression of cGMP. As expected, the 316 L SS and polydopamine groups supported platelet adhesion regardless of the presence of an NO donor (Fig. 3A and Fig. S6A).

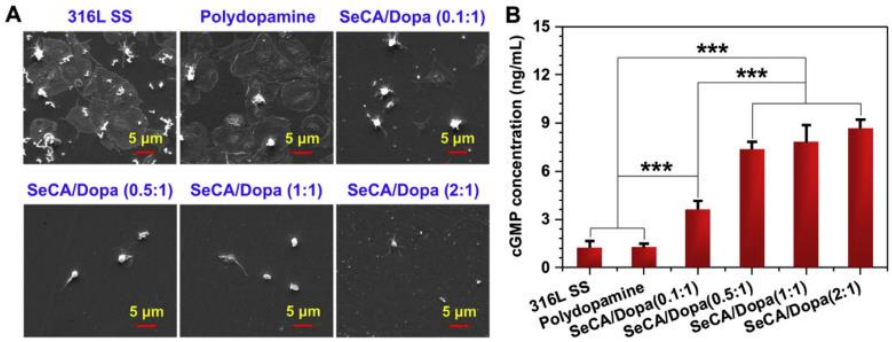

Fig. 3. Adhesion and cGMP expression of platelets incubated in PRP with addition of NO donor. (A) SEM images and (B) cGMP concentration of platelets incubated with 316 L SS, polydopamine and SeCA/Dopa coatings for 30 min. Data presented as mean ± SE (n = 4) and analyzed using a one-way ANOVA (***p < 0.001).

The capability to inhibit adhesion and proliferation of SMCs is crucial to inhibit ISR after stent implantation. The effects of SeCA/Dopa coatings on the growth of SMCs were thus studied. HUASMCs were found to attach to all specimens without donor supplement (Fig. S7). Compared to 316 L SS and pure polydopamine coatings, the SeCA/Dopa coatings showed significant inhibition to HUASMC attachment and migration when supplemented with NO donor (Fig. 4A, Fig. S8). In addition, the SeCA/Dopa coatings were found to dramatically promote the synthesis of cGMP in the presence of an NO donor, and the concentrations of cGMP were highly correlated to the NO flux. The cGMP expression levels were further enhanced in platelets with a higher SeCA-to-Dopa molar ratio, suggesting the bioavailability and bioactivity of NO generated by SeCA/Dopa coatings (Fig. 4B). Moreover, the SeCA/Dopa coating exhibited significant inhibition in proliferation of HUASMCs after 1 and 3 days of culture (Fig. 4C).

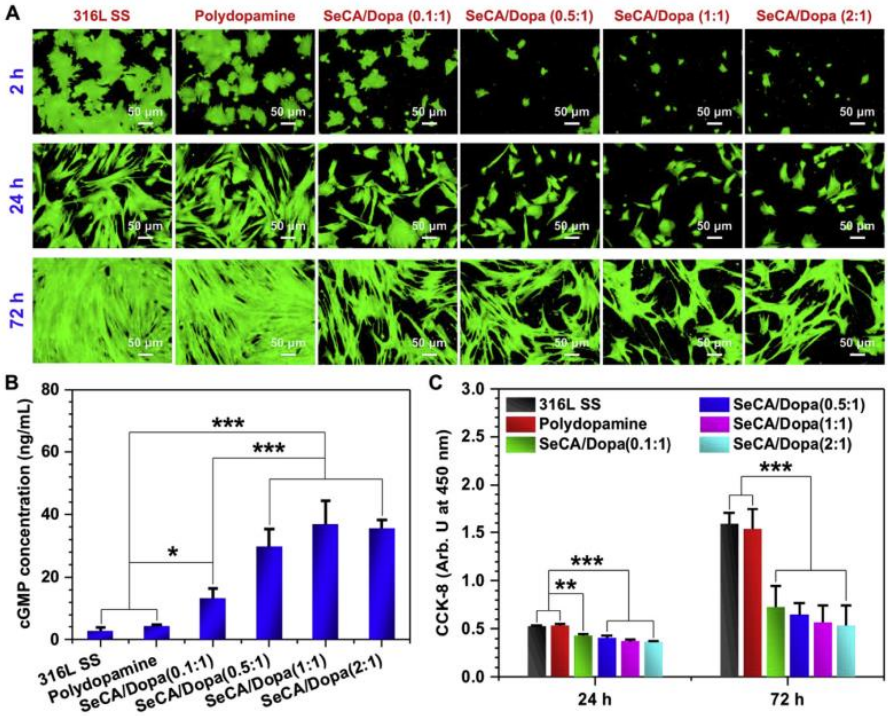

Fig. 4. Adhesion and proliferation of HUASMCs incubated in cell culture media with addition of NO donor. (A) Fluorescence staining of HUASMCs cultured on the 316 L SS, polydopamine and SeCA/Dopa coatings for 2, 24 and 72 h, respectively. (B) cGMP synthesized by HUASMCs cultured on samples for 2 h. (C) Proliferation of HUASMCs on the 316 L SS, polydopamine and SeCA/Dopa coatings after culture for 24 and 72 h. Data presented as mean ± SE (n = 4) and analyzed using one-way ANOVA (*p < 0.05, **p < 0.01, ***p < 0.001).

NO possesses multitudinous physiological effects, including the ability to stimulate EC growth that provides a unique advantage for endothelium repair (endothelium is a natural barrier to prevent thrombosis) [29]. To evaluate the effects of SeCA/Dopa coatings on EC behaviors, HUVECs were cultured on the surface of SeCA/Dopa coatings. It was found that there was no significant difference in the growth behavior of the cells on 316 L SS and polydopamine surfaces in the absence and presence of NO donor (Fig. 5A, Fig. S9). On the contrary, in the presence of NO donor, the increase of cell adhesion and proliferation after 2 h culture of HUVECs revealed that the SeCA/Dopa coatings provided a better microenvironment to support EC attachment, proliferation and migration compared to naked 316 L SS (Fig. 5B–D, Fig. S10). These data suggested that the production of NO induced by SeCA/Dopa coatings supported attachment, proliferation and migration of HUVECs.

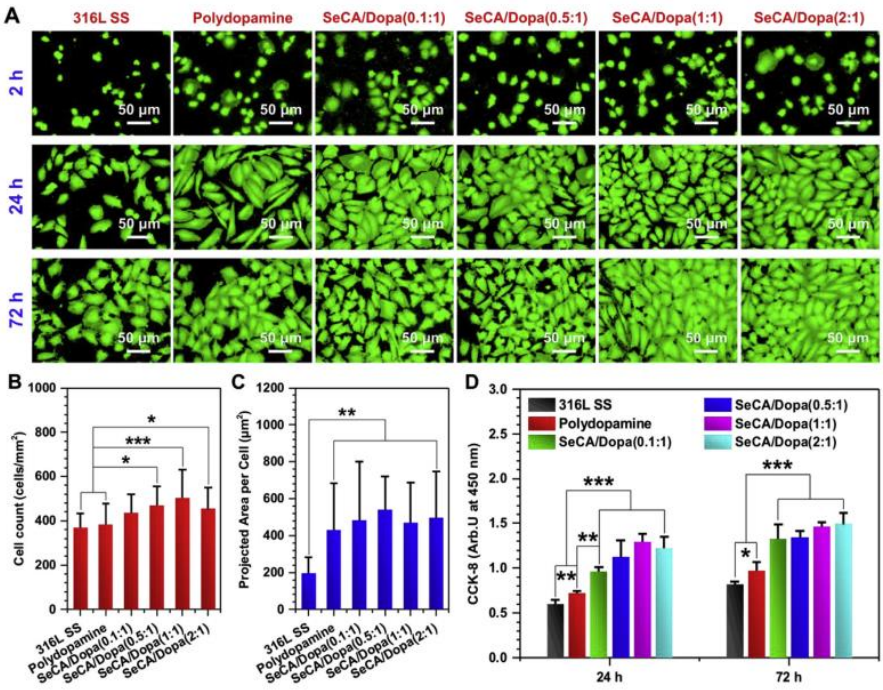

Fig. 5. Adhesion and proliferation of HUVECs incubated in cell culture media with addition of NO donor. (A) Fluorescence staining of HUVECs cultured on the 316 L SS, polydopamine and SeCA/Dopa coatings for 2, 24 and 72 h, respectively. (B) Amounts of HUVECs attached onto samples after culture of 2 h (n = 12). (C) Projected area per cell of HUVECs attached onto samples after culture of 2 h (n = 100). (D) Proliferation of HUVECs grown on the 316 L SS, polydopamine and SeCA/Dopa coatings after culture of 24 and 72 h. Data presented as mean ± SE (n = 4) and analyzed using a one-way ANOVA (*p < 0.05, **p < 0.01, ***p < 0.001).

The competitive behavior between HUVECs and HUASMCs on SeCA/Dopa coatings is a major factor to promote re-endothelialization. To examine the competitive behavior between the cells, HUVECs and HUASMCs were co-cultured on the surface of different samples. A remarkable increase in the amount of HUVECs, with a decrease in HUASMCs, was observed in the presence of an NO donor, especially in higher SeCA/Dopa molar ratio groups (SeCA/Dopa = 2:1) (Fig. S11). In the absence of NO donor, there was no significant difference between the 316 L SS and SeCA/Dopa coatings regarding the number of HUASMCs and HUVECs. These results indicate that the SeCA/Dopa coatings could selectively inhibit SMC attachment, proliferation and migration, while enhancing EC attachment, proliferation and migration. The uniquely selective effects of the NO-generating coatings of SeCA/Dopa on SMCs and ECs endow the SeCA/Dopa-modified stents with the potential to promote the regeneration of a healthy endothelial layer, as well as address the issues of ISR and LST. Based on the above systematic evaluation, the NO-generating SeCA/Dopa coatings with a higher molar ratio of 2:1 showed more desirable NO release and biological effects (i.e., inhibition of adhesion and proliferation of platelets and HUASMCs with simultaneous enhancement of adhesion and proliferation of HUVECs). Taken together, the SeCA/Dopa (2:1) would be an optimized ratio for re-endothelialization and anti-thrombosis, and was thus selected for the following ex and in vivo experiments.

3.4. Thrombogenicity in ex vivo circulation

To demonstrate the anti-thrombogenic properties of SeCA/Dopa coatings in blood, an ex vivo blood circulation experiment was assembled in a New Zealand white rabbit arteriovenous shunt (Fig. 6A). The results revealed a decrease in wall thrombosis after 2 h of flow in SeCA/Dopa-coated 316 L SS foils compared to naked 316 L SS foils (Fig. 6B). Statistical analysis of the occlusions showed that the tubing with an internal installation of the naked 316 L SS foil had a 71.4 ± 11.2% occlusion (calculated by cross-section diameter), whereas no detectable occlusion was found in the

SeCA/Dopa-coated samples (Fig. 6C). The SeCA/Dopa coatings on the 316 L SS foil also led to a significant reduction in occlusive thrombosis (Fig. 6D). The total weight of thrombus harvested from the SeCA/Dopa-coated 316 L SS foil (16.2 ± 5.8 mg) was much lower than that of the thrombus formed on the 316 L SS foil (192.1 ± 21.5 mg) (Fig. 6E). We further evaluated the practicability of circuit with SeCA/Dopa-coated 316 L SS foil to support blood flow. It was noteworthy that the blood flow rate of the circuit with SeCA/Dopa-coated 316 L SS foil remained at 89.3 ± 8.8%, a significantly higher rate than that of the circuit with the control 316 L SS foil (28.9 ± 6.9%) (Fig. 6F). Surface morphology after 2 h of blood circulation was analyzed using SEM to study the effects of SeCA/Dopa coating on platelet adhesion under ex vivo circulation. The results suggested that the SeCA/Dopa coating on 316 L SS foils suppressed platelet activation and fibrin formation (Fig. 6G), indicating effective physiological functions of NO induced by SeCA/Dopa coating in blood flow.

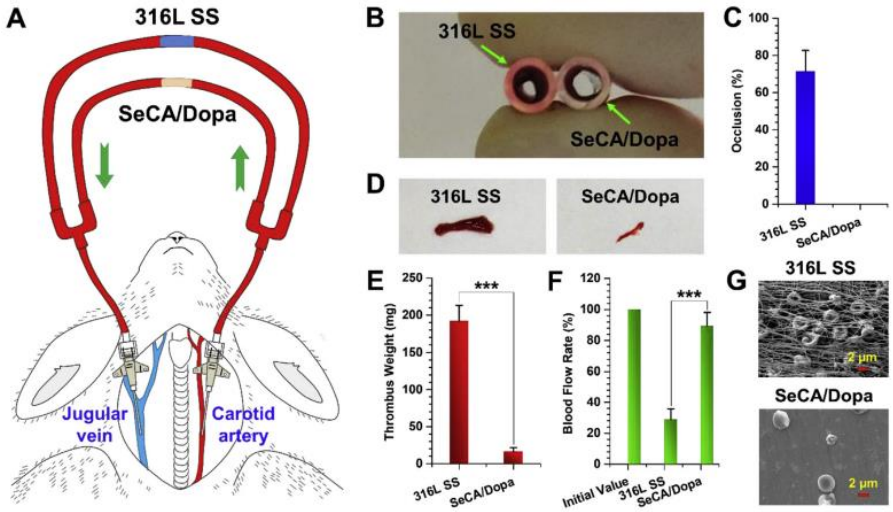

Fig. 6. Thrombogenicity of SeCA/Dopa-coated 316 L SS foils in a New Zealand white rabbit arteriovenous shunt model. (A) The *ex vivo* circulation thrombogenicity model of a rabbit. (B) Cross-sectional photographs of tubing containing 316 L SS foils before and after SeCA/Dopa coatings exposed for 2 h to blood flow in a rapid arteriovenous shunt model without heparin (an important polysaccharide for anticoagulation and inhibition of intimal hyperplasia). (C) Percent occlusion of circuits reveals a significant reduction in occlusion after SeCA/Dopa-modification to 316 L SS foils. (D) Photographs of thrombus formed on 316 L SS foils before and after SeCA/Dopa coating. (E) Thrombus weight of the SeCA/Dopa-coated 316 L SS circuit. (F) Blood flow rate generated using different circuits at the end of *ex vivo* circulation. (G) SEM images of platelet adhesion onto the 316 L SS surface. Data presented as mean ± SE (n = 4) and analyzed using a one-way ANOVA (***p < 0.001).

3.5. In vivo stent implantation

To investigate the feasibility of SeCA/Dopa coatings for promoting re-endothelialization and suppressing restenosis, stent implantations were further performed in rabbit iliac arteries under angiographic control (Fig. S12). The stented iliac arteries were harvested after 1 and 3 months and then analyzed using SEM to evaluate endothelial regeneration (Fig. 7A). ECs were collected and observed on both control and SeCA/Dopa-coated stents after 1 month. The surface of the naked 316 L SS stent was not fully covered by ECs, while a dense EC monolayer completely covered the SeCA/Dopa-coated stent surface. After a longer stent implantation time, intimal hyperplasia was observed on the control stent, evident by the indistinct stent profile. There were some fiber-like tissues growing on the surface of the control stent after 3 months of implantation. By contrast, the intact ECs grew on the SeCA/Dopa-coated stents with a thinner intima and a distinct stent profile. To further understand the effects of SeCA/Dopa-coated stents on ISR, a histomorphometric analysis was carried out (Fig. 7B). The histomorphometric images revealed that the SeCA/Dopa-coated stents significantly reduced neointimal hyperplasia compared to the naked 316 L SS stent. The mean neointimal area (1.9 ± 0.6 mm2 vs 1.3 ± 0.1 mm2) and percentage of neointimal stenosis (39.9 ± 3.2% vs 28.3 ± 5.2%) of SeCA/Dopa-coated stents were remarkably reduced compared to the naked 316 L SS stents after 1 month (Fig. 7C and D). After implantation for 3 months, the mean neointimal area

and the percentage of neointimal stenosis increased to 4.1 ± 0.4 mm2 and 64.1 ± 8.5%, respectively for the 316 L SS stent, whereas little changes were detected in the SeCA/Dopa-coated stents (1.87 ± 0.01 mm2 for the mean neointimal area and 30.9 ± 6.5% for the percentage of neointimal stenosis). These results have demonstrated that the release of NO induced by the SeCA/Dopa-coated stents played an important role in enhancing re-endothelialization and reducing ISR in vivo.

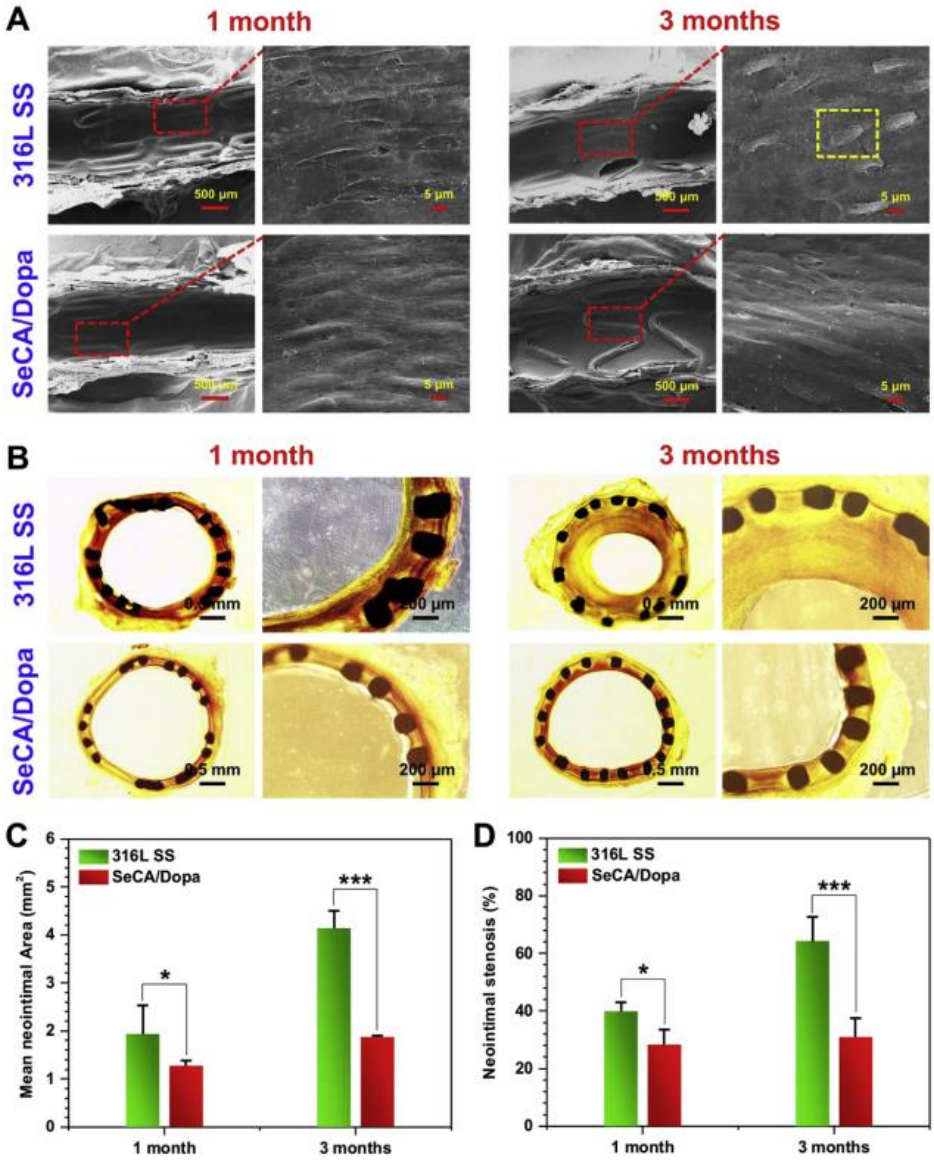

Fig. 7. Cardiovascular stents coated by SeCA/Dopa coating for enhancing re-endothelialization and reducing restenosis. (A) Re-endothelialization of SeCA/Dopa-coated and control 316 L SS stents after implantation for 1 and 3 months observed by SEM. Re-endothelialization was significantly greater on the SeCA/Dopa-coated stent surface compared to the naked 316 L SS stent. (B) The effects of the naked 316 L SS and SeCA/Dopa-coated stents on ISR assessed by histomorphometric analysis. (C) Mean neointimal area and (D) Neointimal stenosis analysis of 316 L SS and SeCA/Dopa-coated stents. Data presented as mean ± SE and analyzed using a one-way ANOVA (*$p < 0.05$, ***$p < 0.001$).

Consequently, the above results have suggested that our SeCA/Dopa coating possesses unprecedented advantages over the existing releasing NO stents which suffer from either burst or insufficient release of NO [10,30] as well as NO-generating stents which is normally associated with tedious and complicated synthesis steps, leakage of toxic chemicals and weak adhesion to stents [24]. Our SeCA/Dopa coating demonstrates a long-term, controllable and stable NO generation within the physiological range, which as a result, leads to impressively improved anti-thrombogenicity, anti-ISR and anti-LST as well as enhanced re-endothelization. Furthermore, it exhibits strong adhesion to cardiovascular stents. We envision that such coating has great potential

in surface chemistry modification of blood-contracting devices.

4. Conclusion

In this work, we have developed a facile “one-pot” technique to synthesize tunable NO-generating coatings through a simple dip-coating of SeCA and Dopa in aqueous solution for promoting re-endothelialization and reducing restenosis and thrombosis. Such a SeCA/Dopa coating enabled us to develop a catalytic surface for local NO generation by reacting the endogenously existing S-nitrothiol species from fresh blood. We found that such SeCA/Dopa coatings exhibited the ability for long-term, stable and adjustable range of NO production rates being unparalleled with any existing NO-generating surface functionalization toolkits. In addition, the SeCA/Dopa coatings with good mechanical properties showed excellent adhesion strength to the stents and inhibited great collagen-induced platelet activation and aggregation. Moreover, the adhesion, proliferation and migration of HUASMCs and HUVECs was significantly suppressed and enhanced by SeCA/Dopa coatings, respectively, and the coatings also supported the competitive growth of HUVECs over HUASMCs. Additionally, the stent implantation results demonstrated that the SeCA/Dopa-coated stents could promote re-endothelialization in vivo. Such a one-step surface modification strategy based on bio-inspired catecholic chemistry would provide an endothelium-mimetic microenvironment, promoting the re-endothelialization on the luminal surface of the cardiovascular stents and potentially addressing the long-term complications including ISR and LST.

Acknowledgements

This work was supported by the National Natural Science Foundation of China (Project 31570957, 81501596 and Key Program 81330031), the Distinguished Young Scholars of Sichuan Province (Project 2016JQ0027), the Fundamental Research Funds for the Central Universities (Project 2682018ZT23) and start-up fund (1-ZE7S) and central research fund (G-YBWS) from the Hong Kong Polytechnic University.

References

[1] R. Waksman, R. Torguson, M.-A. Spad, H. Garcia-Garcia, J. Ware, R. Wang, S. Madden, P. Shah, J. Muller. The lipid-rich plaque study of vulnerable plaques and vulnerable patients: study design and rationale Am. Heart J., 192 (2017), pp. 98-104.

[2] H.M. Mamudu, T.K. Paul, L. Wang, S.P. Veeranki, H.B. Panchal, A. Alamian, K. Sarnosky, M. Budoff The effects of multiple coronary artery disease risk factors on subclinical atherosclerosis in a rural population in the United States Prev. Med., 88 (2016), pp. 140-146.

[3] G.G. Stefanini, D.R. Holmes Jr. Drug-eluting coronary-artery stents N. Engl. J. Med., 368 (3) (2013), pp. 254-265

[4] J.A. Belardi, M. Albertal

Genous™ endothelial progenitor cell capturing stent: thrombus-resistant but vulnerable to restenosis Cathet. Card

[5] F. Otsuka, A.V. Finn, S.K. Yazdani, M. Nakano, F.D. Kolodgie, R. Virmani The importance of the endothelium in atherothrombosis and coronary stenting Nat. Rev. Cardiol., 9 (8) (2012), pp. 439-

[6] C. Liang, Y. Hu, H. Wang, D. Xia, Q. Li, J. Zhang, J. Yang, B. Li, H. Li, D. Han Biomimetic cardiovascular stents for in vivo re-endothelialization Biomaterials, 103 (2016), pp. 170-182.
[7] T. Unoki, H. Wada, M. Akao, S. Ura, A. Yamada, K. Takabayashi, Y. Yamashita, Y. Hamatani, N. Masunaga, M. Ishii Serum vascular endothelial growth factor-C Levels are inversely associated with the risk of cardiac and cerebrovascular events following drug-eluting stent implantation Circulation, 130 (2014) A13044–A13044
[8] J.H. Yoon, C.J. Wu, J. Homme, R.J. Tuch, R.G. Wolff, E.J. Topol, A.M. Lincoff Local delivery of nitric oxide from an eluting stent to inhibit neointimal thickening in a porcine coronary injury model Yonsei Med. J., 43 (2) (2002), pp. 242-251.
[9] X. Gu, Z. Mao, S.-H. Ye, Y. Koo, Y. Yun, T.R. Tiasha, V. Shanov, W.R. Wagner Biodegradable, elastomeric coatings with controlled anti-proliferative agent release for magnesium-based cardiovascular stents Colloids Surfaces B Biointerfaces, 144 (2016), pp. 170-179.
[10] M.A. Elnaggar, S.H. Seo, S. Gobaa, K.S. Lim, I.H. Bae, M.H. Jeong, D.K. Han, Y.K. Joung Nitric oxide releasing coronary stent: a new approach using layer-by-layer coating and liposomal encapsulation Small, 12 (43) (2016), pp. 6012-6023.
[11] L.J. Ignarro Nitric oxide: a unique endogenous signaling molecule in vascular biology (Nobel lecture) Angew. Chem. Int. Ed., 38 (13–14) (1999), pp. 1882-1892
[12] N. Naghavi, A. de Mel, O.S. Alavijeh, B.G. Cousins, A.M. Seifalian Nitric oxide donors for cardiovascular implant applications Small, 9 (1) (2013), pp. 22-35.
[13] M.W. Vaughn, L. Kuo, J.C. Liao Effective diffusion distance of nitric oxide in the microcirculation Am. J. Physiol. Heart Circ. Physiol., 274 (5) (1998), pp. H1705-H1714
[14] A. Tan, D. Goh, Y. Farhatnia, N.G.,J. Lim, S.-H. Teoh, J. Rajadas, M.S. Alavijeh, A.M. Seifalian An anti-CD34 antibody-functionalized clinical-grade POSS-PCU nanocomposite polymer for cardiovascular stent coating applications: a preliminary assessment of endothelial progenitor cell capture and hemocompatibility PLoS One, 8 (10) (2013), p. e77112.
[15] J.S. Beckman, W.H. Koppenol Nitric oxide, superoxide, and peroxynitrite: the good, the bad, and ugly Am. J. Physiol. Cell Physiol., 271 (5) (1996), pp. C1424-C1437
[16] W.A. Pryor, G.L. Squadrito The chemistry of peroxynitrite: a product from the reaction of nitric oxide with superoxide Am. J. Physiol. Lung Cell Mol. Physiol., 268 (5) (1995), pp. L699-L722
[17] J.W. Yoo, J.S. Lee, C.H. Lee Characterization of nitric oxide-releasing microparticles for the mucosal delivery J. Biomed. Mater. Res., 92 (4) (2010), pp. 1233-1243
[18] A. de Mel, N. Naghavi, B.G. Cousins, I. Clatworthy, G. Hamilton, A. Darbyshire, A.M. Seifalian Nitric oxide-eluting nanocomposite for cardiovascular implants J. Mater. Sci. Mater. Med., 25 (3) (2014), pp. 917-929.
[19] J. An, S. Chen, J. Gao, X. Zhang, Y. Wang, Y. Li, S. Mikhalovsky, D. Kong, S. Wang Construction and evaluation of nitric oxide generating vascular graft material loaded with organoselenium catalyst via layer-by-layer self-assembly Sci. China Life Sci., 58 (8) (2015), pp. 765-772.
[20] W. Cha, M.E. Meyerhoff Catalytic generation of nitric oxide from S-nitrosothiols using immobilized organoselenium species Biomaterials, 28 (1) (2007), pp. 19-27.
[21] Z. Yang, Q. Tu, M.F. Maitz, S. Zhou, J. Wang, N. Huang Direct thrombin inhibitor-bivalirudin functionalized plasma polymerized allylamine coating for improved biocompatibility of vascular devices Biomaterials (32) (2012), pp. 7959-7971.

[22] J. Waite Mussel beards: a coming of age Chem. Ind., 2 (1991), pp. 607-611
[23] H. Lee, S.M. Dellatore, W.M. Miller, P.B. Messersmith Mussel-inspired surface chemistry for multifunctional coatings Science, 318 (5849) (2007), pp. 426-430.
[24] Z. Yang, Y. Yang, K. Xiong, X. Li, P. Qi, Q. Tu, F. Jing, Y. Weng, J. Wang, N. Huang Nitric oxide producing coating mimicking endothelium function for multifunctional vascular stents Biomaterials, 63 (2015), pp. 80-92
[25] S. Goldstein, J. Lind, G. Merényi Chemistry of peroxynitrites as compared to peroxynitrates Chem. Rev., 105 (6) (2005), pp. 2457-2470.
[26] Y. Yang, P. Qi, F. Wen, X. Li, Q. Xia, M.F. Maitz, Z. Yang, R. Shen, Q. Tu, N. Huang Mussel-inspired one-step adherent coating rich in amine groups for covalent immobilization of heparin: hemocompatibility, growth behaviors of vascular cells, and tissue response ACS Appl. Mater. Interfaces, 6 (16) (2014), pp. 14608-14620.
[27] J.S. Isenberg, M.J. Romeo, C. Yu, K.Y. Christine, K. Nghiem, J. Monsale, M.E. Rick, D.A. Wink, W.A. Frazier, D.D. Roberts Thrombospondin-1 stimulates platelet aggregation by blocking the antithrombotic activity of nitric oxide/cGMP signaling Blood, 111 (2) (2008), pp. 613-623
[28] S.S. Ahanchi, N.D. Tsihlis, M.R. Kibbe The role of nitric oxide in the pathophysiology of intimal hyperplasia J. Vasc. Surg., 45 (6) (2007), pp. A64-A73.
[29] L.J. Taite, P. Yang, H.W. Jun, J.L. West Nitric oxide-releasing polyurethane-PEG copolymer containing the YIGSR peptide promotes endothelialization with decreased platelet adhesion J. Biomed. Mater. Res. B Appl. Biomater., 84 (1) (2008), pp. 108-116
[30] G.T. El-Ferzli, A. Andukuri, G. Alexander, M. Scopel, N. Ambalavanan, R.P. Patel, H.W. Jun A nitric oxide-releasing self-assembled peptide amphiphile nanomatrix for improving the biocompatibility of microporous hollow fibers American Society for Artificial Internal Organs, 61 (5) (2015), pp. 589-595